

The Effect of Light on the Epitranscriptome of Plants

Sophia Jang

1. Introduction

As the global population increases and crops are detrimentally affected by different climatic factors, producing enough food to meet global demand is a primary concern. According to the Food and Agriculture Organization of the United Nations (FAO), about 70% more food is required to feed the expected population of over nine billion people by 2050, which requires a 37% increase over the historical annual incremental rates (Mba, 2013). However, this necessity is hindered by several factors. For example, arable land and agricultural water resources are limited and already insufficient in parts of the developing world due to urbanization and the competitive obligations to produce livestock, energy, and products of other industries (Mba, 2013). This insufficiency is only exacerbated by the harmful effects that climate change has on arable land (Mba, 2013). However, although farmers are using more agrochemicals, their usage is not sustainable in the long run because they have been shown to be harmful to public health and the environment, and the genetic uniformity within crops induces greater vulnerability in the first place to the same threats (Mba, 2013).

Due to these factors, methods that can produce food with fewer resources must be developed. One potential path for sustainable crop production intensification is through studying how to genetically modify plants' responses to light. Proper light perception is essential to many plants' survival, as light perception controls plant functions aligned with seasonal time, developmental timing, geographic location, and functions such as flowering. In addition, photosynthesis utilizes light to provide the main source of energy for green organisms (Artz, et al., 2019). Studying the effectiveness of photosynthesis and the molecular mechanisms of light receptors is therefore important for the cultivation of agricultural crops. Plants have evolved different traits that enhance their likelihood to survive, including flowering in reaction to red light, seasonal and geographical cues, and secondary metabolites such as caffeine and nicotine. Elucidating the biomolecular and genetic mechanisms that specifically alter plants' adaptations, and how these can be modified, would greatly contribute to the necessary knowledge for sustainable crop production intensification.

Two main growth patterns have been determined in most land plants: photomorphogenesis and skotomorphogenesis (Figure 1). Photomorphogenic plants grow in response to light, developing shorter hypocotyls, (etiolation) and unfurling embryonic leaves. Skotomorphogenic light development is in the absence of light, and plants displaying this development pattern form an apical hook that is bent to protect the cotyledon, which contains important meristem cells (Moglich, Yang, Ayers, & Moffat, 2010) necessary for plant growth, and can be identified by their extended hypocotyls (which indicate de-etiolation). Hypocotyls elongate in an effort to reach light for the seedling's development (Josse & Halliday, 2008).

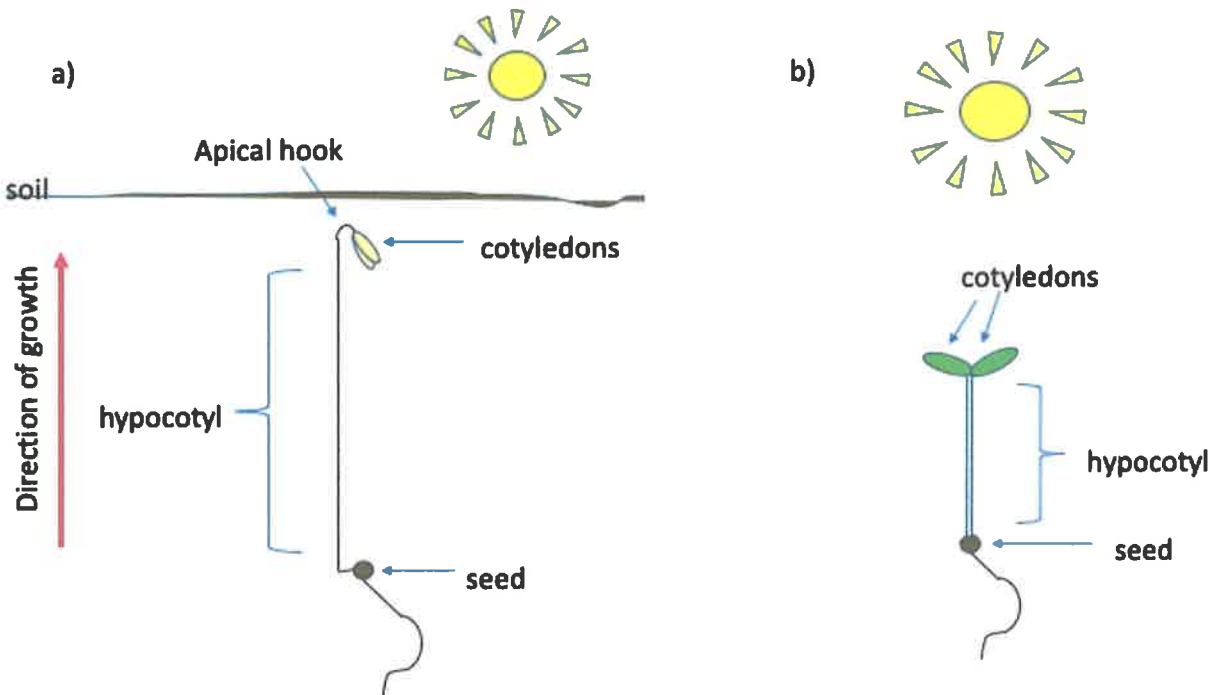


Figure 1 Plants can either display a development pattern typically seen in the absence of light, skotomorphogenesis (a) or in the presence of light, photomorphogenesis (b). Plants undergoing skotomorphogenesis differ with the development of an apical hook that allows the plant to grow in perceived darkness by pushing through soil implicated to be separating the plant from access to light. This is aided by the elongation of the hypocotyl, or de-etiolation, which retracts nutrients from the cotyledons, resulting in their yellow color (Created by student researcher).

An agricultural detriment of skotomorphogenic plants is accelerated reproductive development, resulting in lower biomass and seed yield (Casal, 2012). Therefore, studying how to minimize de-etiolation is important for crop optimization. Light has also been found to be responsible for regulating tissue-autonomous promotion of palisade cell development (Kozuka et al., 2011), and palisade cells are essential for the utilization of light for photosynthesis and therefore maximum energy production by plants. Through these studies, potential genetic targets for energetic optimization of crop plants can be identified, and thereby how to produce more crops with fewer resources or under less optimal conditions.

Within plants, there are many different photoreceptors, such as phytochromes, phototropins, and others, each of which responds to specific ranges of light wavelength (Figure 2). Therefore, when studying specific functions that result from the absorbance of light by different photoreceptors, it is important to study model plants under the corresponding wavelength of light. Cryptochromes, which are photoexcited by blue light, are a major photoreceptor of interest as they are responsible for seedling de-etiolation (short stem elongation), flowering time, and shade avoidance (Artz, et al., 2019). The sensitivity of the etiolation response to the absence of light is vital towards studying shade avoidance, in which densely packed plants, such as those in agricultural fields, react not to light but the absence of light, extending their hypocotyls to reach sunlight. Understanding how these photoreceptors interact to produce

the de-etiolation phenotype is therefore important for cultivating healthier agricultural crops in greater numbers on less arable land.

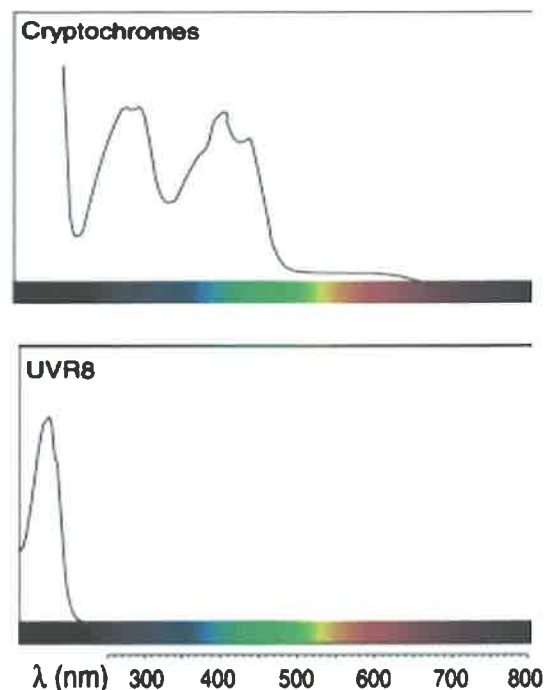


Figure 2 Graphs of absorbance for different photoreceptors. These graphs depict the wavelength ranges that different photoreceptors may absorb light in. Phototropins and zeitlupes absorb blue and green light best, cryptochromes absorb blue light best, as do UVRs. However, unique to phytochromes are their ability to absorb red light and far red light (Created by Galvao & Fankhauser, 2015).

Cryptochromes are present in both plants and vertebrates, with similar functions across the different eukaryote groups. In mammals, the cryptochromes have been shown to perform as light-independent components of the circadian clock, and they are also photoreceptors for the circadian clock in *Drosophila* (Griffin, Staknis, & Weitz, 1999). For example, cryptochromes are responsible for clock function, such as preparing for photosynthesis before the first sun rays in the morning, plant growth, flowering, de-etiolation, stress response, temperature regulation, and changing conformation in reaction to blue light. In vertebrates and insects, cryptochromes do not act as photoreceptors but do demonstrate some response to light, contributing to proper circadian rhythm, the repression of gene expression, magnetoperception, metabolism and cancer, and sun compass navigation.

Cryptochromes are photoexcited by blue light, and therefore are of interest to studying de-etiolation when seedlings are deprived of blue light. Cryptochrome 2, or CRY2, is specifically degraded when exposed to high fluence rates of light (Yu, et al., 2007). Since CRY2 has been found to encourage

de-etiolation by regulating PIF activity in blue light, it has been hypothesized that under low blue light, PIF5 is abundant, initiating interactions with CRY1/CRY2 to promote plant growth (Pedmale, et al., 2016). In terms of the specific mechanisms of regulating other photoreceptors, CRY2 has also been hypothesized to localize to chromatin (Pedmale, et al., 2016), which consists of protein, RNA, and DNA. If CRY2 is able to directly regulate the activity of other photoreceptors, changes to the surrounding environment of crops can induce phenotypic changes (Pedmale, et al., 2016), which may determine the successful growth of crops.

Arabidopsis thaliana is often utilized in dicotyledon studies of photoreceptors and other plant physiology studies. Using this species is greatly advantageous given the publication of its entire genome sequence and the many more publications on its function and structure in comparison to other flowering plants (Koornneef & Meinke, 2010). Other advantages include its relatively small genome size compared to most crop species, which often have larger genomes than humans, its short generation time, small size which is ideal for limited growth facilities, and prolific seed production through self-pollination (Koornneef & Meinke, 2010). This allows for relatively quick cultivation of a large number of model plants to study and for the sequencing of extracted genetic material.

According to the Rice Genome project, *Arabidopsis* generally appears to share the same large gene classes as most crop species, with discrepancies being due to polyploidy of crop species. The polyploidy of crop species indicates repeated sets of chromosomes rather than many unique DNA sequences, so its similarity to other crop plants makes it ideal for agricultural studies on plants such as cabbage and mustard (Koornneef & Meinke, 2010). The Columbia (Col) accession, or ecotype, is used as it is generally accepted as the reference genotype based on past studies incorporating microarray data, mutant collections, and other biochemical information (Koornneef & Meinke, 2010).

A protein of interest for studying de-etiolation in *Arabidopsis* is ECT2, or evolutionarily conserved C-terminal region 2. Past research has indicated that it regulates gene expression, by assisting in the transfer of cytosolic calcium signals to cell nuclei (Ok, et al., 2005). It has recently been implied that this induces the same phenotype as CRY2, but it is yet unknown whether these two proteins interact with the other to induce de-etiolation.

ECT2 is specifically of interest because of its relationship with m⁶A, or N⁶-methyladenosine. The RNA-protein complex that results from m⁶A has been demonstrated to contribute to many critical RNA modifications and functions such as the nuclear export of RNA, splicing of introns, translation, RNA stability, and localization. Prior to the discovery of this RNA modification, most were known to be static, in contrast to m⁶A. However, it has also been discovered that m⁶A can be demethylated (Jia, et al., 2011). Moreover, while it has not been found in genomic DNA of higher eukaryotes, it has been clearly identified in cellular mRNAs isolated from all higher eukaryotes (Jia, et al., 2011), which encompasses

plants. Since mRNA is the basic construct in the cell for producing polypeptides, and thereby proteins, modifications of mRNA should directly impact the expression of proteins, such as photoreceptors. In addition, demethylation specifically can mask parts of the genome and expose only promoters, thereby modifying the proteins produced and how they function (Ooi & Bestor, 2008). CRY2 may reside in chromatin in order to actively modify the activity of other photoreceptors, which supports the concept that m⁶A mechanisms may be directly impacting the expression of CRY2.

Currently, the only function determined in plants for m⁶A to have is in RNA stability (Anderson, et al., 2018). So, whether m⁶A also greatly impacts RNA translation in plants as it does in animals is of great interest.

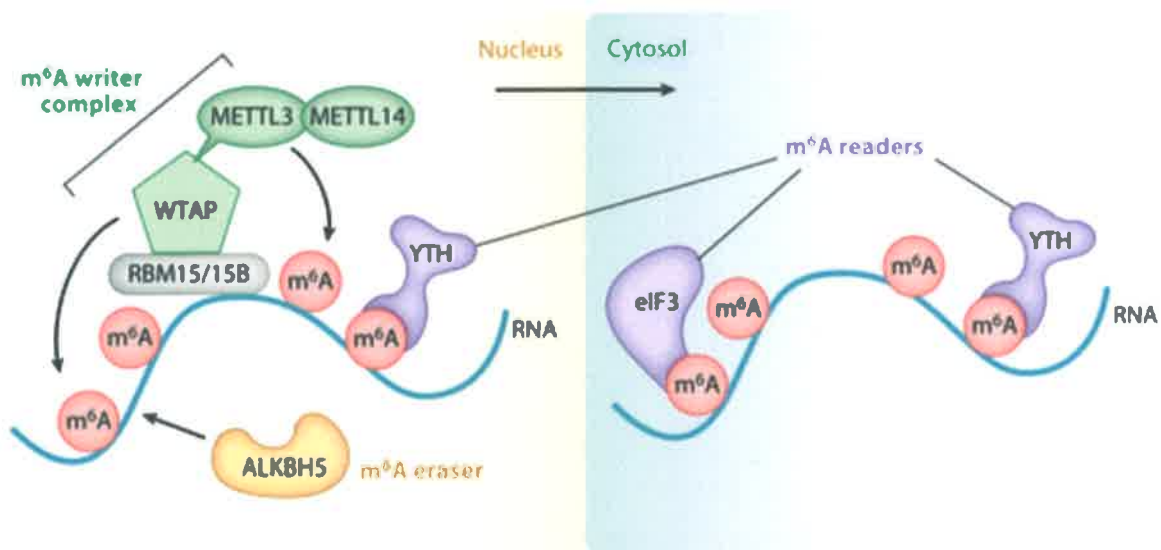


Figure 3 A diagram demonstrating the physiology of the m⁶A RNA-protein complex. There are three main writers, or methyltransferases, in plants that deposit methyl on RNA, as well as demethylases, or erasers, and m⁶A readers. These readers bind to m⁶A and recruit other proteins, including ECT2. These proteins can induce the degradation or modification of RNA (Created by Meyer & Jaffrey, 2017).

The objective of the project was to confirm that in *Arabidopsis thaliana* *ect2* induces a similar phenotypic effect to *cry2*, and whether the two pathways interact with each other during phenotypic expression.

2. Methodology

2.1 Preparing Seed Aliquots for Hypocotyl Measurements

One sterile Falcon 50 mL conical centrifuge tube was filled with 100% ethanol. A second sterile Falcon 50 mL conical centrifuge tube was filled with 35 mL of 100% ethanol and 15 mL of distilled water, producing a 70% ethanol mixture. 50 µL of Triton X-100 detergent was added to the 70% ethanol mixture to destroy the surface tension of the water.

Approximately fifty seeds of the Columbia (Col) accession from each of the genotypes Col-0 (the wildtype), *cry1*, *cry2*, *cry1cry2*, and *ect2* were aliquoted into five individual autoclaved 1.7 mL Eppendorf tubes. 800 μ L of the 70% ethanol was transferred with the P2000 pipette to each aliquot in order to partially sterilize the seeds. The seed aliquots were then rotated in a VWR tube rotator for ten minutes.

The 70% ethanol was then immediately removed with a P2000 pipette under a flow hood to ensure sterile conditions. 800 μ L of the 100% ethanol was added to each seed aliquot, and the Eppendorf tubes were rotated for five minutes. The P2000 pipette was then used to remove the ethanol under the flow hood from each Eppendorf tube, and 500 μ L of distilled water was added to each seed aliquot. Each Eppendorf tube was then inverted several times in order to ensure that there was an even saturation of any remaining ethanol, and that not only seeds at the bottom were soaked in any remaining ethanol, which would negatively affect germination. The water was pumped in and out of the pipette as the Eppendorf tube was held sideways, so that the seeds settled along one side of the tube.

Three square Petri dishes were labelled so that one row on each Petri dish corresponded to one genotype, thus there were five rows for WT, *cry1*, *cry2*, *cry1cry2*, and *ect2*. The P2000 pipette was set to 400 μ L for the 500 μ L in each Eppendorf tube to prevent air bubbles, and drew up seeds along the side of the Eppendorf tube. The pipette was held vertically so that the dense seeds gathered in the bottom of the pipette tip. Approximately fifteen seeds were then dispensed per row to the corresponding genotype on each of the three Petri dishes by touching the surface of the Murashige and Skoog (MS) medium on the Petri dishes.

Each of the Petri dishes were sealed shut with sterile surgical tape and then wrapped in two layers of aluminum foil to block out possible white light to prevent premature germination. The plates were then placed in continual darkness at 4°C for three days to simulate winter conditions to stimulate germination. For the third trial, this methodology was slightly modified to include a sixth seed aliquot, another sample of *ect2* that was confirmed to possess the mutation. The remainder of the original *ect2* aliquot that was not confirmed to possess the proper mutation was used to dispense eight seeds on a fourth Petri plate.

2.2 Growing *Arabidopsis* Plants in Blue Light

The Petri dishes were removed from the cold room. The probe of light meter was inserted in the growth chamber, and the blue light adjusted with the control panel until the light meter read approximately 10 μ mol/ m^2 /s for the first trial, and then the aluminum foil was removed from the Petri dishes in the growth chamber. The seedlings remained in the growth chamber for five days. For the second trial and third trial, the light meter was adjusted to 1.0 μ mol/ m^2 /s. For the first trial, one Petri

dish was placed vertically on a ledge in the growth chamber and the other two Petri dishes were placed flat on the ledge.

2.3 Hypocotyl Assay

After the Petri dishes were removed from the growth chamber, the lids were removed and a pair of tweezers was used to gently push the plants flat against the agar, parallel to the bottom of the dish. The Petri dishes were then placed face down on an Epson flat scanner and images were saved as TIF files. ImageJ was then used to measure the hypocotyls of each plant for each genotype. The resulting data was saved and analyzed with Excel. T-tests were conducted using the Excel function between desired genotypes, and the standard deviation was also found to take standard error into account.

2.4 Bacterial Inoculation

Luria-Bertani (LB) medium plates were made. This was to determine whether the agrobacteria to be used to infiltrate tobacco retained its genetic integrity by possessing functional barnase inhibitors of the barnase genes. Otherwise, these damage synthesized RNA before secretion and thereby kill the bacteria. The antibiotics rifampicin, gentamycin, and kanamycin were removed from the fridge, and were placed to thaw on a heat block at 37°C, or human body temperature, which is the optimal temperature for these antibiotics.

LB agar was microwaved and poured into three 50 mL Falcon tubes under a flow hood. 50 µL of each antibiotic was dispensed into separate Falcon tubes (antibiotics are concentrated 1000x). The Falcon tubes were then mixed by being inverted approximately ten times each. The mixture from each Falcon tube was then poured onto separate round Petri dishes, and the dishes were left to solidify for twenty minutes.

Agrobacteria were then dispensed on each Petri dish lid with a pipette, and the pipette tip was bent perpendicular to the pipette. The bacteria were spread with the bent tip around the agar on the Petri dish, and left to inoculate overnight. Inoculating bacteria in only water is generally avoided. This is when water freezes, crystals may damage the bacteria, therefore cryoprotectants such as glycerol are useful.

2.5 Preparing the MES Buffer for Tobacco Infiltration

A stir bar was placed in a clean 500 mL beaker. The beaker was filled with 400 mL of deionized and filtered water, and then placed on the magnetic stirrer. A sterile plastic boat was placed on the balance and the mass was set to 0.0 grams, and a spatula was then used to scoop 0.48 grams of MES (2-ethanesulfonic acid) hydrate into the plastic boat. 0.48 grams were used to produce a 10 mM MES solution of volume 500 mL.

The MES hydrate was dispensed in the 500 mL beaker on the magnetic stirrer, and the spatula was disposed of and the plastic boat thrown out. A second sterile plastic boat was placed on the balance

and the mass set to 0.0 grams, and a clean spatula was used to scoop 0.98 grams of magnesium chloride into the plastic boat. The magnesium chloride was dispensed in the solution in the 500 mL beaker on the magnetic stirrer. The pH meter probe was rinsed with distilled water, and potassium hydroxide was gradually added until the pH was adjusted to 5.6.

2.6 Tobacco Infiltration

After the bacteria were incubated, they were removed from the cold room and spun down in a centrifuge at 3800 rpm for fifteen minutes. Then the supernatant was discarded from each sample. A 50 mL aliquot of the 500 mL of MES buffer was set aside. Then, the bacteria were resuspended in MES buffer and incubated for one hour in semi-dark conditions.

The three tobacco plants were well watered to induce stomata to open one hour before the experiment.

After the bacteria were incubated, they were spun down in the centrifuge at 3800 rpm for fifteen minutes and the supernatant was discarded from each sample. The bacteria were resuspended in MES buffer. Then, three different combinations were mixed. Each mixture received 2 mL of cV-ect2, and 1 mL of p19, the anti-silencing strain. Each mixture received 1 mL of either nvCRY1, nvCRY2, or nv-mock.

A 1.0 mL HSW syringe was used to infiltrate the abaxial side of the tobacco leaves, selecting leaves that were not too old or too young, and that were large in surface area. One plant received the mixture with nvCRY1, one plant received the mixture with nvCRY2, and the third plant received the mixture with nv-mock.

2.7 Yellow Fluorescence Protein Analysis of Tobacco Plants

One of the three tobacco plants was selected at a time for analysis. An entire leaf was cut off of the petiole with a razor blade, and 2 drops of water were pipetted onto a clean glass slide. Then a square was cut from the area of the tobacco leaf that was previously infiltrated with the syringe. The square sample was placed on the glass slide with tweezers over the water droplets, so that the underside was facing upward in order to ensure proper analysis by the microscope. A cover slip was then placed over and gently flattened on the sample using the backside of the tweezers.

An EVOS FL microscope was used to analyze each sample. It was turned on, and first set to transmitted light, then switched to the setting appropriate for yellow fluorescent protein. A cover was placed over the stage of the microscope to block out surrounding light, and the image was brought into focus. True fluorescence could first be surmised with the presence of bright dots in cells' nuclei, then confirmed by increasing objective power, which reveals if the fluorescence is merely from ultra-fluorescence in trichomes rather than true fluorescence in the nucleus. Pictures were taken using the "capture" button.

2.8 Gateway Cloning of m⁶A Writers – LR Reaction

Two 1.5 mL Eppendorf tubes were labelled and set aside on ice. The entry clones and destination vectors were spun down in the centrifuge for 3-5 seconds, then also put on ice. The P2 micropipette was then used to transfer 2 μ L of the corresponding entry clones to MTA and FIP37 each, and 2 μ L of the corresponding destination vectors to MTA and FIP 37. The 5x LR Clonase II was removed from the fridge, and flicked lightly, before being centrifuged for 3 seconds. The P2 micropipette was then used to pipette 1 μ L of the LR Clonase II into each of the two Eppendorf tubes. Then, the tubes were spun down for 1 second, then incubated for 1 hour at room temperature.

0.5 μ L of ProteinaseK was then added with the P1 micropipette. 2 aliquots of TOP10 Chemically Competent *E. coli* were removed from -80 °C and left to thaw for ten minutes in an ice bucket. The 5 μ L of LR Clonase II Enzyme Mix for MTA and FIP37 were then added to separate *E. coli* aliquots. LB agar was set on ice, and the two samples were placed in the Eppendorf ThermoMixer C for 45 seconds. The samples were returned to the ice for 2 minutes. 800 μ L of LB was added to each of the two samples using the P1000 micropipette. The bacteria were finally transferred to Falcon tubes and left in the New Brunswick incubator shaker for forty minutes.

2.9 Preparation for Colony PCR

20 μ L of distilled water was pipetted into each of the eight PCR tubes of one PCR tube strip. The Petri dish with the bacterial colonies that had been transformed with the MTA expression clones was opened, and the PCR tubes remained open. A colony was touched by the pipette tip of the P2000 pipette, in order to gently pick up the bacteria, and then the pipette tip was ejected into the first PCR tube. This was done for four colonies. This process with the bacterial colonies was repeated for the FIP37 expression clones. The plate was shaken around, and then the bacteria in the water were resuspended, but not for too much time, in order to maintain structural integrity for PCR. The PCR tubes were then left to cool in a deli cooler to 4°C.

2.10 Plasmid DNA Miniprep for Sequencing

The New England BioLabs Monarch Plasmid DNA Miniprep Kit was used to prepare the gateway cloning products for each writer for sequencing. 24 mL of ethanol was added to the 6 mL of given wash buffer. 1-5 mL of bacterial culture was pelleted by centrifugation for 30 seconds. The supernatant was afterward discarded. The pellet was then resuspended in 200 μ L, and subsequently pipetted to ensure complete suspension and thus effective lysis (a Vortex or pipette may be used).

The bacterial cells were lysed by adding 200 μ L Plasmid Lysis Buffer with the P1000 micropipette. The tube was immediately gently inverted approximately five times, but not vortexed, until the color turned dark pink and the solution was clear and viscous. For the remainder of this procedure, the cells were not vortexed due to instability and the possibility of rupturing. The lysate was neutralized by adding 400 μ L of Plasmid Neutralization Buffer with the P1000 micropipette, and the tube then inverted until the

color was uniformly yellow and a precipitate (proteins) formed. The bacteria were then incubated for 2 minutes.

The lysate was centrifuged for 2-5 minutes at 16,000 x g. The longer the spin time, the more compact the pellet that formed which minimized the risk of clogging the column. The supernatant was then transferred to the spin column by pouring it in, and centrifuged for 1 minute. The flow-through was discarded, leaving behind only large proteins and DNA. The column was reinserted in the collection tube, and 200 µL of Plasmid Wash Buffer 1 was added in order to remove the RNA, protein, and endotoxin. The column was then centrifuged for 1 minute at full speed.

400 µL of Plasmid Wash Buffer 2 was carefully added with the P1000 micropipette, so that no liquid touched the filter as ethanol on the filter would precipitate DNA. The column was then centrifuged for 1 minute at top speed. The column was then transferred to a clean 1.5 mL microfuge tube. Then at least 30 µL of DNA Elution Buffer was added to the center of the matrix, the column was left to sit for a minute, and then spun for a minute to elute the DNA.

2.11 Measuring DNA Density with the Spectrophotometer

The NanoDrop One/One Microvolume UVU-Vis Spectrophotometer was turned on. The option “Nucleic acids” was selected on the menu, then “dsDNA” (doubled stranded DNA due to the plasmids), and then “Self test”. The arm of the spectrophotometer was raised, then a P2 micropipette was used to load 1.5 µL of the blank, elution buffer, onto the bottom pedestal to set the base concentration value for buffer without any DNA. The arm was put down, and after the concentration was automatically measured, both pedestals were wiped clean with a Kim wipe. Then, each sample was loaded onto the pedestal, wiping both pedestals in-between sample measurements.

2.12 Bacterial Transformation Electro Competent Cell (Electroporation)

The plasmid was thawed in an ice bucket. The bacteria were removed from -80 °C and put on ice for 3-5 minutes until thawed. 1 µL of diluted plasmid was added to the cells, and the cell and plasmid mix (approximately 55 µL) was carefully to a clean cuvette with a micropipette, so that the material was touching both plates. By inserting the pipette tip in-between electrolytes, this helped to ensure a relatively even dispersal of the mixture, and a steady insertion helped reduce bubbles.

The electroporator (BioRad MicroPulser) was turned on and set to the AgR setting for agrobacteria and the maximum time (2.5). The first cuvette was completely dried with a paper towel before being placed in the electroporator, and the two red buttons were pushed at the same time and released after the beep (approximately 2-3 seconds after pressing the buttons). To check that the electroporator successfully worked, the display should read 6-6.5 after pressing “Time Const.”

Immediately after removing the cuvette from the electroporator, ½ mL LB was added to the cuvette, and pipetted in and out several times. Then the entire content of the cuvette was pipetted into a sterile 1.5

mL Eppendorf tube, and the cuvette disposed of. This process was repeated for each cuvette. Afterward, the cells were incubated for approximately 1 hour at 37 °C.

There were three possible methods for plating the bacteria after incubation. The first was simply pipetting the desired amount onto LB agar containing antibiotics on a Petri dish. The second method required more steps. The tube with the bacteria and LB was centrifuged at 5000 RPM for 5 minutes, then the supernatant was poured off. The pellet was resuspended in 50 μ L LB, and the cell solution pipetted onto an LB plate with the desired antibiotic. Then a spreader was removed from ethanol, held over the Bunsen burner to burn off the ethanol, allowed to cool for a couple of seconds, and touched to the agar before being used to spread the cells. The resulting plate then sat at 37 °C overnight.

For the third method, the 55 μ L was pipette onto a Petri dish, and glass beads were added and shook around. The plate was left to dry in a flow hood before being placed upside down in a 37 °C incubator overnight. Afterward, the plate was stored at 4 °C when sealed with parafilm.

3. Results

3.1 Initial Hypocotyl Assay

In the first trial, the genotypes WT (wildtype), *cry1*, *cry2*, *cry1cry2*, and *ect2* were grown under 1 μ mol/m²/s blue light. The average measurements of CRY2 and ECT2 were similar to that of wildtype (Figure 4a). A t-test was conducted between all the values for hypocotyl length for the CRY2 genotype across the three Petri dishes and all the values for the WT genotype across the three Petri dishes, producing a p-value of 0.6764338, greater than 0.05 and therefore not significant. However, a t-test conducted between all the values for hypocotyl length for the ECT2 genotype across the three Petri dishes and all the values for the WT genotype across the three Petri dishes produced a very significant p-value of 1.00405E-05. Since the average hypocotyl length of the ECT2 genotype was smaller than the average hypocotyl length of the WT genotype (Figure 4a), it was indicated that the ECT2 genotype produces a very hypersensitive response to light, stronger than the WT, as the shorter hypocotyl length is characteristic of photomorphogenic plants. However, the results of the t-test between the CRY2 values and the WT values indicate that the *cry2* photoreceptor is not as vital for the photomorphogenic response in high blue light.

In the second trial, the average hypocotyl lengths of the ECT2 and CRY2 genotypes were again similar to those of the WT genotype (Figure 4b), with short hypocotyls characteristic of the photomorphogenic response. A t-test was conducted between all the values for hypocotyl length for the CRY2 genotype across the three Petri dishes and all the values for the WT genotype across the three Petri dishes, producing a p-value of 0.330164, greater than 0.05 and therefore insignificant. However, a t-test conducted between all the values for hypocotyl length for the ECT2 genotype across the three Petri dishes

and all the values for the WT genotype across the Petri dishes produced a very significant p-value of 3.71236E-08.

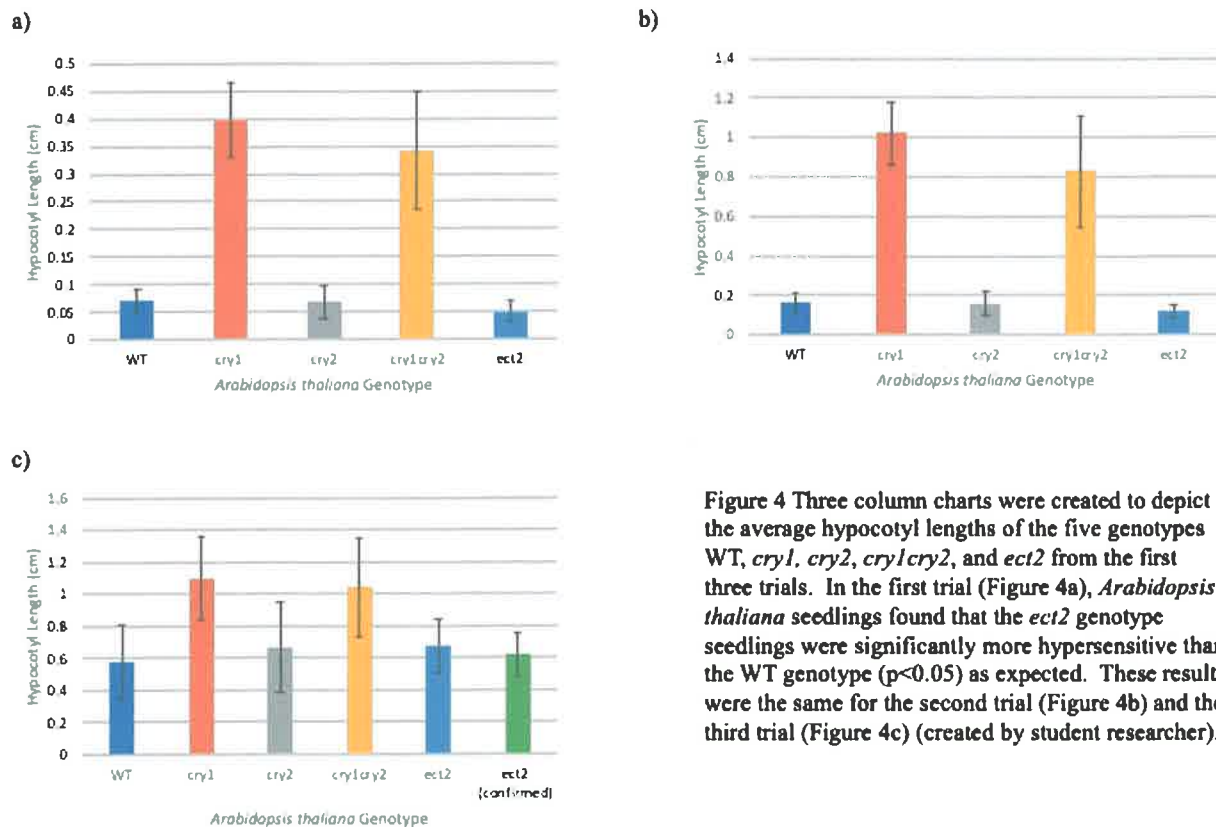


Figure 4 Three column charts were created to depict the average hypocotyl lengths of the five genotypes WT, *cry1*, *cry2*, *cry1cry2*, and *ect2* from the first three trials. In the first trial (Figure 4a), *Arabidopsis thaliana* seedlings found that the *ect2* genotype seedlings were significantly more hypersensitive than the WT genotype ($p < 0.05$) as expected. These results were the same for the second trial (Figure 4b) and the third trial (Figure 4c) (created by student researcher).

This not only correlates with the hypothesis that the ECT2 genotype produces a similar phenotype to the CRY2 genotype, but that it actually induces a more hypersensitive response than the CRY2 genotype does.

The third trial was conducted to confirm the results of the second trial. As expected, the average hypocotyl lengths of the ECT2 and CRY2 genotypes were similar to those of the WT genotype (Figure 4c), with shorter hypocotyls characteristic of the photomorphogenic response. A t-test was conducted between all the values for hypocotyl length for the CRY2 genotype across the three Petri dishes and all the values for the WT genotype across the three Petri dishes, producing a p-value of 0.099774, greater than 0.05 and therefore insignificant. However, a t-test conducted between all the values for hypocotyl length for the ECT2 genotype across the three Petri dishes and all the values for the WT genotype across the Petri dishes produced a significant p-value of 0.01060999. These results support the results from the second trial.

3.2 Infiltration of Tobacco Plants

Eighteen photos were taken of the tobacco plants under yellow light. The cluster of fluorescent nuclei in the tobacco leaf infiltrated with ECT2 and CRY2 fragments (Figure 5) indicated that these two protein pathways interacted with each other, as each protein was bound to one half of a yellow fluorescent protein (YFP) (Figure 5). However, the fluorescent cytoplasm visible in the tobacco leaf infiltrated with ECT2 and WT fragments (mock) with an absence of any fluorescence in nuclei indicated that yellow fluorescent protein has a tendency to bind together when in close proximity, and therefore the procedure's validity was falsified. Therefore, a new procedure to approach investigating the interaction of the protein pathways must be created.

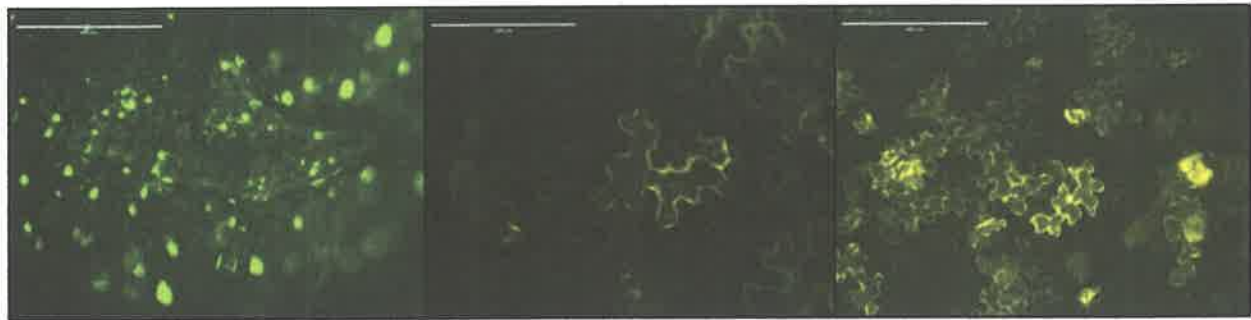


Figure 5 The fluorescent images above depict the vectors for ECT2 and mock (control), ECT2 and CRY2, and ECT2 and CRY1, respectively. The fluorescence for ECT2 and mock and ECT2 and CRY1 are false positives, given that true fluorescence from the binding of the two halves of the protein ought to only occur in the nuclei (created by student researcher).

3.3 Hypocotyl Length Analysis with Darkness Controls

Due to the results of the first three trials of hypocotyl measurements of the *Arabidopsis thaliana* genotypes, which were slightly inconsistent but generally showed the *ect2* genotype to be significantly more hypersensitive than the *cry2* genotype in comparison to the wildtype, seedlings were grown in darkness as a control to confirm this phenotypical trend. The fourth trial compared the five genotypes grown in the same length of simulated winter, and then in either darkness or blue light of $1.0 \mu\text{mol}/\text{m}^2/\text{s}$ (Figure 6a). Unexpectedly, the *ect2* genotype produced shorter seedlings in darkness than the wildtype genotype did. It would have been expected that there would not be a significant difference between the hypocotyl lengths across genotypes grown in darkness because with no light exposure, there should be no differences in growth initiated by different hypersensitivities to light.

In the fifth trial, another experimental factor was added. The five genotypes for the *Arabidopsis* seedlings were grown on two Petri plates for each group of darkness, a $0.5 \mu\text{mol}/\text{m}^2/\text{s}$ fluence rate of blue light, and a $1.0 \mu\text{mol}/\text{m}^2/\text{s}$ fluence rate of blue light (Figure 6b). As expected, there was no significant difference between the hypocotyl lengths of the *cry2* and WT genotypes for either blue light fluence rates.

However, contrary to suggested hypersensitivity in the first three trials, there was no significant difference between the *ect2* and WT genotypes either for either blue light level. Another unexpected result was that the *cry1* and *cry1cry2* genotypes had shorter hypocotyls than the WT genotype in darkness. It would be expected that without any light to initiate hypersensitivity, seedlings would not produce shorter hypocotyls in response to light.

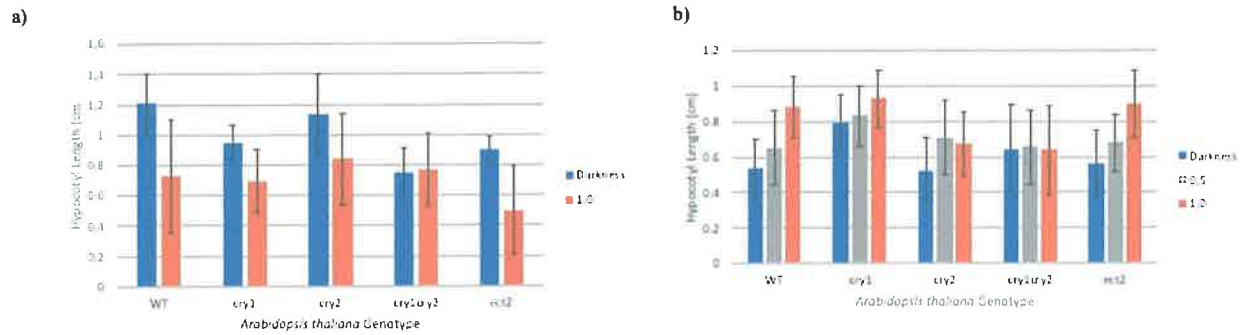


Figure 6 Two column charts were created to depict the average hypocotyl lengths of the five genotypes WT, *cry1*, *cry2*, *cry1cry2*, and *ect2* in both darkness and blue light. In the fourth trial, *Arabidopsis thaliana* seedlings were grown in darkness and a blue light fluence rate of $1.0 \mu\text{mol}/\text{m}^2/\text{s}$, and the *ect2* genotype seedlings were significantly shorter and therefore more hypersensitive than the WT genotype ($p < 0.05$) in darkness (Figure 6a). In the fifth trial, *Arabidopsis thaliana* seedlings were grown under an additional condition, under a blue light fluence rate of $0.5 \mu\text{mol}/\text{m}^2/\text{s}$, and *ect2* seedlings were not significantly more hypersensitive than WT seedlings in either blue light condition ($p > 0.05$) (created by student researcher).

There are two possible explanations for the de-etiolation of the *cry2* and *cry1cry2* genotypes. It is possible, but not likely that the *cry2* gene is therefore important for the development of the plant itself, which would suggest a novel importance of the cryptochrome photoreceptor proteins. However, it is more likely that there is an issue with the germination of the seed line itself. This would require further investigation and the usage of a new seed line for future experiments with the *Arabidopsis* genotype seedlings.

In the sixth hypocotyl assay trial, two plates of the *Arabidopsis thaliana* genotypes WT, *cry1*, *cry2*, and *cry1cry2* were grown in $0.5 \mu\text{L}/\text{m}^2/\text{s}$ of blue light and two plates were grown in darkness for five days (Figure 7). Both groups received a white light pulse for an hour midway during the growth period, to induce germination of the seeds. However, germination rates were calculated at the end of the growth periods (Figure 7a). The germination rates for the first plate grown in blue light were 0.8888889, 1.000000, 0.89473684, and 0.941176747 for the genotypes WT, *cry1*, *cry2*, and *cry1cry2*, respectively. The germination rates for the second plate grown in blue light were 0.9, 0.94117647, 0.82352941, and 0.88888889 for the genotypes WT, *cry1*, *cry2*, and *cry1cry2* respectively. The germination rates for the first plate grown in darkness were 0.94736842, 0.50, 0.61, and 0.53 for the genotypes WT, *cry1*, *cry2*, and *cry1cry2*, respectively. The germination rates for the second plate grown in darkness were 0.70588235, 0.55555556, 0.61111111, and 0.38888889 for the genotypes WT, *cry1*, *cry2*, and *cry1cry2* respectively.

In comparison, two plates of seedlings of the same genotype were grown in darkness for the seventh hypocotyl assay trial, and were exposed to a longer white light pulse of six hours. The germination rates improved with the longer white light pulse. The germination rates for the first plate were 1, 0.95, 1, and 1 for the genotypes WT, *cry1*, *cry2*, and *cry1cry2*, respectively. The germination rates for the second plate were 0.94444444, 0.95, 1, and 0.88888889 for the genotypes WT, *cry1*, *cry2*, and *cry1cry2* respectively. The hypocotyl lengths were also more consistent between the different genotypes in darkness than they were for Trial #6 (Figure 7d, 7b).

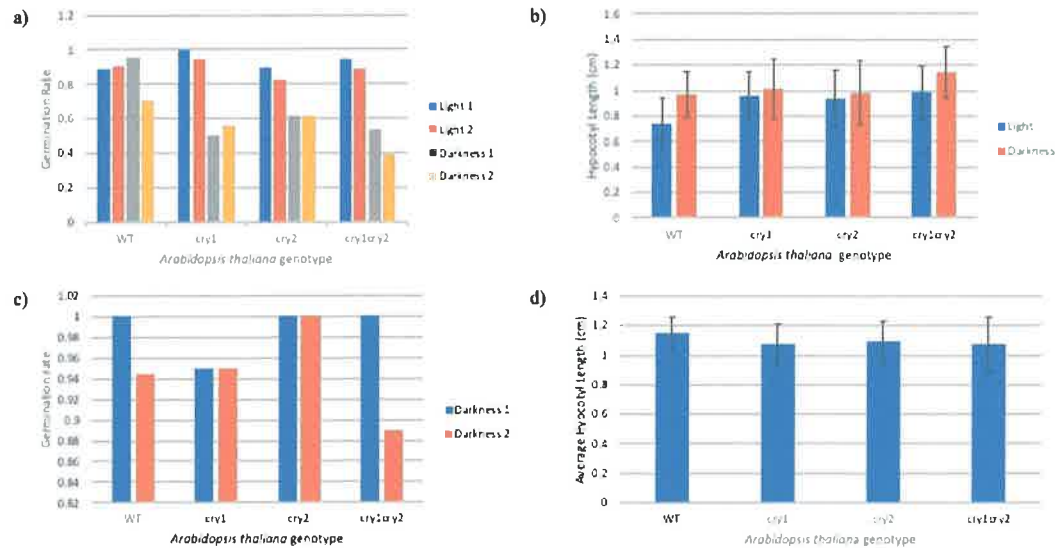


Figure 7 Four column charts were created to depict average hypocotyl length and germination rate for the four genotypes WT, *cry1*, *cry2*, and *cry1cry2*. Poor germination rates were observed for one hour of white light pulse in Trial 6 (Figure 7a), so the white light pulse was extended to six hours for Trial 7 (Figure 7b), which demonstrated far higher germination rates. The positive impact of improved germination rates on the accuracy hypocotyl assays is implied by the far more consistent hypocotyl lengths across different genotypes in darkness in Trial 7 (Figure 7d) in comparison to the genotypes grown in darkness in Trial 6 (Figure 7b) (created by student researcher).

For the eighth trial of the hypocotyl assay, two plates of *Arabidopsis thaliana* were grown in blue light and two plates were grown in darkness. All four plates had the genotypes WT, *cry1*, *cry2*, and *cry1cry2*, and were exposed to a white light pulse of 8.5 hours (in comparison to the 6 hours in Trial 7 and the 1 hour in Trial 6). The seedlings that were grown in darkness did not have significantly different average hypocotyl lengths across the different genotypes. A t-test was conducted between the WT genotype and each of the other genotypes, producing p-values of 0.052386254, 0.66202705, and 0.13595267 for *cry1*, *cry2*, and *cry1cry2*, respectively. There was a significant difference between the average hypocotyl length of WT and *cry2* under blue light, with a t-test producing a p-value of 5.48977E-11, $p < 0.05$.

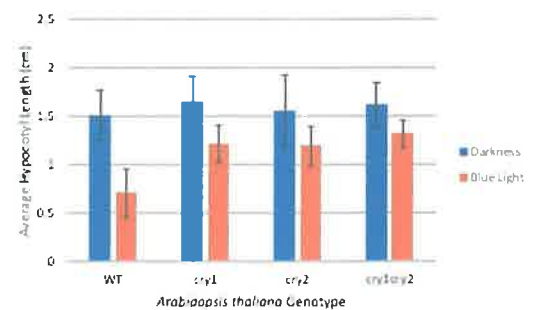


Figure 8 A column chart depicting the average hypocotyl lengths of the *Arabidopsis thaliana* genotypes WT, *cry1*, *cry2*, and *cry1cry2* was constructed. After exposure to 8.5 hours of white light to initiate germination, none of the genotypes had significantly different average hypocotyl lengths ($p > 0.05$). *cry2* demonstrated significantly less hypersensitivity to blue light ($p < 0.05$) (created by student researcher).

4. Discussion

4.1 Hypocotyl Assays

In order to determine whether *ect2* produces a similar phenotypic effect in *Arabidopsis thaliana* to *cry2*, *Arabidopsis thaliana* serving as a model plant, etiolation was identified through hypocotyl assays. Since CRY2 is known to inhibit hypocotyl elongation, the genotype *cry2*, which lacks the CRY2 photoreceptor, would be expected to exhibit skotomorphogenic growth, where etiolation is present and hypocotyls are elongated. If *ect2* produces a similar phenotype to *cry2*, then both should produce *Arabidopsis thaliana* seedlings with significantly greater hypocotyl length than the wildtype seedlings under blue light. However, CRY2 protein is known to be degraded under high fluence rates of blue light (Pedmale, et al., 2016). Thus, whether *cry2* would appear hypersensitive or hyposensitive under blue light is expected to vary with the fluence rate induced. It was hypothesized that the *ect2* genotype would mirror each phenotypic expression of the *cry2* genotype.

In the first trial, the seedlings were grown under a relatively high blue light fluence rate of 1.0 $\mu\text{mol}/\text{m}^2/\text{s}$, resulting in only *ect2* seedlings that demonstrate significantly more hypersensitivity than WT, and not *cry2*. It would have been anticipated that both would have displayed significantly more hypersensitivity. This is especially so for *cry2*, since it would be degraded. If *cry2* was degraded, skotomorphogenic growth in response to darkness may not have been present. Therefore, the seedlings would have been expected to demonstrate photomorphogenic growth, or shorter hypocotyls, as being appropriate for a hypersensitivity to blue light. However, in the second trial, the seedlings were grown under a relatively low blue light (LBL) fluence of 0.5 $\mu\text{mol}/\text{m}^2/\text{s}$. As expected, *cry2* did not demonstrate hypersensitivity, whereas *ect2* did. The third trial was also grown under the same LBL, resulting in the *ect2* seedlings having significantly ($p < 0.05$) taller hypocotyls, which was expected for Trial 2. Part of this was attributed to uncertainty about whether the *ect2* aliquot was actually a mutant *ect2* aliquot. Thus, an aliquot from a different line was incorporated into Trial 3 (“*ect2* (confirmed)” in Figure 4c).

Trials 4 and 5 repeated the same hypocotyl assay, but produced results inconsistent with known mechanisms. In trial 4, *ect2* seedlings were found to be significantly more hypersensitive than the WT seedlings in darkness. In trial 5, *cry2* was significantly shorter than the WT seedlings in darkness. These results indicated a possible issue with the growth preparation or the seed line itself, since with no blue light in darkness to induce hypersensitivity in mutant seedlings, there should not have been significant differences in hypocotyl lengths across the different genotypes. This was resolved for the following trials, as different white light pulses were utilized for Trials 6-8, until clear results between *cry2* and WT were visible with a much longer initiation of germination, 8.5 hours rather than 1 hour.

4.2 BiFC Procedure

The presence of fluorescence throughout cells indicates that there is a natural affinity for the split YFP1 to remain connected despite splitting the fluorescent protein. Instead of this biomolecular fluorescence complementation (BiFC), BLC can be investigated as an alternative procedure. BLC uses luciferase, with CRY1, CRY2, and mock as vectors as well. The lack of false positives in the resulting images would confirm its validity. An alternative method is using the fluorescent protein mCherry, which can be combined with both CRY2 and ECT2 in seedlings. These can then be grown and imaged. This would allow for the determination of localization – the exact tissues, cells, and organelles of interaction could be seen in fluorescent images. It would be expected that this procedure with mCherry can produce “speckles”, subnuclear structures. Images can be taken with the same Epson microscope used for the BiFC procedure, except under red light.

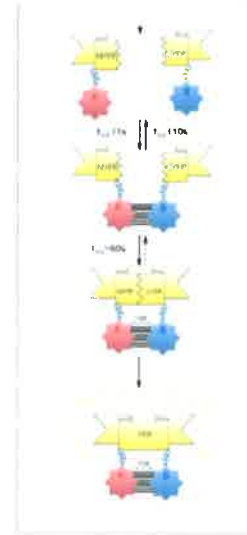


Figure 9 A diagram portraying the methodology for the yellow fluorescence protein infiltration of tobacco plants with vectors in agrobacteria. This was then falsified as a reliable methodology due to false positive results in the controls (Created by Oliver Artz).

4.5 Future Works

To further confirm the phenotypical expression of *ect2*, the *ect2* genotype can be directly compared with an ECT2 overexpressor line, since the absence of the ECT2 protein in the *ect2* genotype should create a less severe skotomorphogenic response compared to the overexpression of the ECT2 protein. The skotomorphogenic response can be quantified by plating seedlings under the same conditions for the two seed lines, and then scanning the Petri dishes. The angle of the apical hook can then be measured using the scanned images. It would be expected that there is a less severe apical hook for the *ect2* genotype than the ECT2 overexpressors.

In order to confirm evidence that CRY2 acts on a pathway through ECT2 for the modification of RNA, the three main writers for m⁶A (MTA, FIP37, and MTB) can be cloned through gateway cloning. These can then be inserted in the entry vector pDONR 221, for infiltration via agrobacteria. This would allow for a biomolecular analysis of the interaction of CRY2 with the three main writers, and different fluorophores can be used to produce corresponding images.

Conclusion

In recent years, there has been renewed interest in the dynamic modification system of m⁶A. As yet, identification of potential applications of the epitranscriptome for future sustainable crop product intensification as just begun.

Significant differences between the genotypes *ect2* and WT, and the genotypes *cry2* and WT were established, implying that *ect2* and *cry2* induce the same phenotype for de-etiolation in *Arabidopsis thaliana*. In attempting to further assess underlying interactions between the two pathways, a well-established procedure for determining protein-protein interactions in plants, YFP, was falsified in this context. This is important for future studies on *ect2*, which has yet to be studied in depth in plants and will likely incur greater interest for both future plant development and plant adaptation studies. The causes for the inconsistency of this method should be studied in the future, in order to properly determine what factors may produce false positive results when studying protein-protein interactions for these photoreceptors with ECT2.

Another broader question that requires clarification is how epitranscriptome modifications can be integrated into agricultural efforts in the future. Genetic modifications are undoubtedly a major approach. The Joint Division of the Food and Agriculture Organization of the United Nations and the International Atomic Energy Agency (Joint FAO/IAEA) has already been introducing mutant rice and other plant varieties suitable for minimizing mineral deficiencies, managing diabetes and obesity, and formulating baby food (Mba, 2013). This is an important development. Although much more research is needed before epitranscriptome research can be fully integrated into agricultural efforts, there are immense potential benefits that dynamic changes to the genetic material can offer.

Bibliography

- Anderson, S. J., Kramer, M. C., Gosai, S. J., Yu, X., Vandivier, L. E., Nelson, A. D., . . . Gregory, B. D. (2018). N-Methyladenosine Inhibits Local Ribonucleolytic Cleavage to Stabilize mRNAs in Arabidopsis. *Cell reports*, 25(5), 1146-1157.
- Artz, O., Dickopf, S., Ranjan, A., Kreiss, M., Abraham, E. T., Boll, V., . . . Hoecker, U. (2019). Characterization of spa mutants in the moss *Physcomitrella* provides evidence for functional divergence of SPA genes during the evolution of land plants. *New Phytologist*.
- Casal, J. J. (2012, January 18). Shade avoidance. *The Arabidopsis Book*, 10.
- Galvao, V. C., & Fankhauser, C. (2015, October). Sensing the light environment in plants: photoreceptors and early signaling steps. *Current Opinion in Neurobiology*, 34, 46-53.
- Griffin, E. A., Staknis, D., & Weitz, C. J. (1999). Light-Independent Role of CRY1 and CRY2 in the Mammalian Circadian Clock. *Science*.
- Jia, G., Fu, Y., Zhao, X., Dai, Q., Zheng, G., Yang, Y., . . . He, C. (2011). N6-methyladenosine in nuclear RNA is a major substrate of the obesity-associated FTO. *Nature Chemical Biology*, 7(12), 885-887.
- Josse, E.-M., & Halliday, K. J. (2008). Skotomorphogenesis: The Dark Light of Light Signalling. *Current Biology*, 18(24), R1144-R1146.
- Koornneef, M., & Meinke, D. (2010). The development of Arabidopsis as a model plant. *The Plant Journal*, 61, 909-921.
- Li, J.-F., Bush, J., Xiong, Y., Li, L., & McCormack, M. (2011). Large-Scale Protein-Protein Interaction Analysis in Arabidopsis Mesophyll Protoplasts by Split Firefly Luciferase Complementation. *PLoS ONE*, 6(11).
- Mba, C. (2013). Induced Mutations Unleash the Potentials of Plant Genetic Resources for Food and Agriculture. *Agronomy*, 3(1), 200-231.
- Meyer, K. D., & Jaffrey, S. R. (2017). Rethinking m 6 A Readers, Writers, and Erasers. *Annual Review of Cell and Developmental Biology*, 33, 319-342.
- Mockler, T., Yang, H., Yu, X., Parikh, D., Cheng, Y.-c., Dolan, S., & Lin, C. (2003, February 18). Regulation of photoperiodic flowering by Arabidopsis photoreceptors. *Proceedings of the National Academy of Sciences of the United States of America*, 100(4), 2140-2145.
- Moglich, A., Yang, X., Ayers, R. A., & Moffat, K. (2010). Structure and Function of Plant Photoreceptors. *Annual Review of Plant Biology*, 61, 21-47.
- Ok, S., Jeong, H., Bae, J., Shin, J.-S., Luan, S., & Kim, K.-N. (2005). Novel CIPK1-Associated Proteins in Arabidopsis Contain an Evolutionarily Conserved C-Terminal Region that Mediates Nuclear Localization. *Plant Physiology*, 138-150.
- Ooi, S. K., & Bestor, T. H. (2008). The Colorful History of Active DNA Demethylation. *Cell*, 133(7), 1145-1148.
- Pedmale, U. V., Huang, S.-s. C., Zander, M., Cole, B. J., Hetzel, J., Ljung, K., . . . Chory, J. (2016, January). Cryptochromes Interact Directly with PIFs to Control Plant Growth in Limiting Blue Light. *Cell*, 164(1-2), 15-17.
- Yu, X., Klejnott, J., Zhao, X., Shalitin, D., Maymon, M., Yang, H., . . . Lin, C. (2007). Arabidopsis Cryptochrome 2 Completes Its Posttranslational Life Cycle in the Nucleus. *The Plant Cell*, 19, 3146-3156.